

Use of Metadynamics in the Design of isoDGR-Based $\alpha\beta 3$ Antagonists To Fine-Tune the Conformational Ensemble**

Andrea Spitaleri, Michela Ghitti, Silvia Mari, Luca Alberici, Catia Traversari, Gian-Paolo Rizzardi,* and Giovanna Musco*

The integrin family of cell-adhesion receptors regulates cellular functions crucial to the initiation, progression, and metastasis of solid tumors. In particular, integrin $\alpha\beta 3$ plays a key role in endothelial cell survival and migration during tumor angiogenesis.^[1] It is therefore gaining increasing importance as a drug target in antiangiogenic cancer therapy.^[2,3] The sequence Arg-Gly-Asp (RGD), which is contained in natural $\alpha\beta 3$ interactors, such as vitronectin, fibronectin, fibrinogen, osteopontin, and tenascin, is by far the most prominent ligand to promote specific cell adhesion through stimulation. This sequence is therefore attractive as a lead for the development of different integrin antagonists.^[4] Recent biochemical studies showed that deamidation of the NGR sequence gives rise to isoDGR, a new $\alpha\beta 3$ -binding motif.^[5] This sequence constitutes a novel class of peptidic integrin ligands and paves the way to drug-design studies with a focus on the synthesis and characterization of a new generation of isoDGR-based macrocycles.^[6,7]

For the design of low-molecular-mass isoDGR-containing molecules, an accurate determination of their biologically active conformation is a prerequisite. The presence of the β bond induces high flexibility in isoDGR-containing macrocycles and thus augments the range of accessible interconverting conformations.^[8] However, the identification of relevant conformations that might affect binding affinity is challenging for standard spectroscopic and diffraction techniques. Atomistic simulations, such as molecular dynamics (MD), replica-exchange molecular dynamics (REMD), and Monte Carlo (MC) simulations, can complement experimen-

tal data.^[9,10] However, they often fail to generate reliable equilibrium conformations because of the rugged and complex nature of the free-energy surface (FES) that is accessible to the system. As a consequence, computational sampling is often relegated to some local, unrealistic minima, which compromise subsequent docking studies. As computational drug design becomes increasingly reliant on virtual screening and on high-throughput 3D modeling, the need for fast and accurate computational methods for sampling of the ensemble of energetically accessible conformations is warranted. In this context, several techniques, including the local-elevation method,^[11] taboo search,^[12] the Wang–Landau method,^[13] adaptive force bias,^[14] conformational flooding,^[15] umbrella sampling,^[16] weighted histogram techniques,^[17] transition-state theory, and path sampling,^[18] have been developed to address the sampling problem, through either reconstruction of the free energy or the direct acceleration of events that might happen on a long timescale (“rare events”). Related to these methods, metadynamics (MetaD)^[19,20] has emerged as a powerful coarse-grained non-Markovian molecular-dynamics approach for the acceleration of rare events and the efficient and rapid computation of multidimensional free-energy surfaces as a function of a restricted number of degrees of freedom, named collective variables (CVs). If the CVs are appropriately chosen for the system under investigation, MetaD directly provides a good estimate of the free energy of the system projected into the CVs (see the Supporting Information for details). Notably, the free energy is not immediately deducible by other sampling methods, such as umbrella sampling, in which the free-energy profile is not obtained directly from the simulations and requires an additional computational step, such as the weighted histogram analysis method (WHAM).^[16]

In this study, we developed a protocol based on the combination of MetaD and docking simulations^[21,22] to analyze the conformations and the $\alpha\beta 3$ -binding properties of isoDGR-containing cyclopeptides and to predict the conformational effects of chemical modifications and discriminate binders from nonbinders in silico. To investigate the conformational equilibrium of RGD-, DGR-, and isoDGR-containing cyclopeptides (cyclization mode involving cysteine side chains) and to exhaustively explore their FESs, we performed well-tempered MetaD simulations,^[23] for which we chose Gly ϕ and ψ angles as CVs (Figure 1; for simulation details, see the Supporting Information).

As it lacks a side chain, Gly has large conformational freedom around its backbone dihedral angles. Therefore, Gly can explore a considerably larger area in the Ramachandran energy diagram than any other amino acid, and occupies five

[*] Dr. A. Spitaleri, Dr. M. Ghitti, Dr. S. Mari, Dr. G. Musco
Dulbecco Telethon Institute, Biomolecular NMR Laboratory
c/o Center of Genomic and Bioinformatics
S. Raffaele Scientific Institute
via Olgettina 58, 20132 Milan (Italy)
Fax: (+39) 02-2643-4153
E-mail: giovanna.musco@hsr.it
L. Alberici, Dr. C. Traversari, Dr. G.-P. Rizzardi
MolMed SpA
via Olgettina 58, 20132 Milan (Italy)
Fax: (+39) 02-2127-7322
E-mail: paolo.rizzardi@molmed.com

[**] This research was supported in part by a research grant from the Italian Ministry of Research (FIRB). We thank Dan Zhou for technical assistance and Renato Longhi for peptide synthesis. We are grateful to Prof. Wilfred van Gunsteren, Dr. M. Bonomi, F. L. Gervasio, and Dr. A. Barducci for useful discussions.

Supporting information for this article, including experimental details, is available on the WWW under <http://dx.doi.org/10.1002/anie.201007091>.

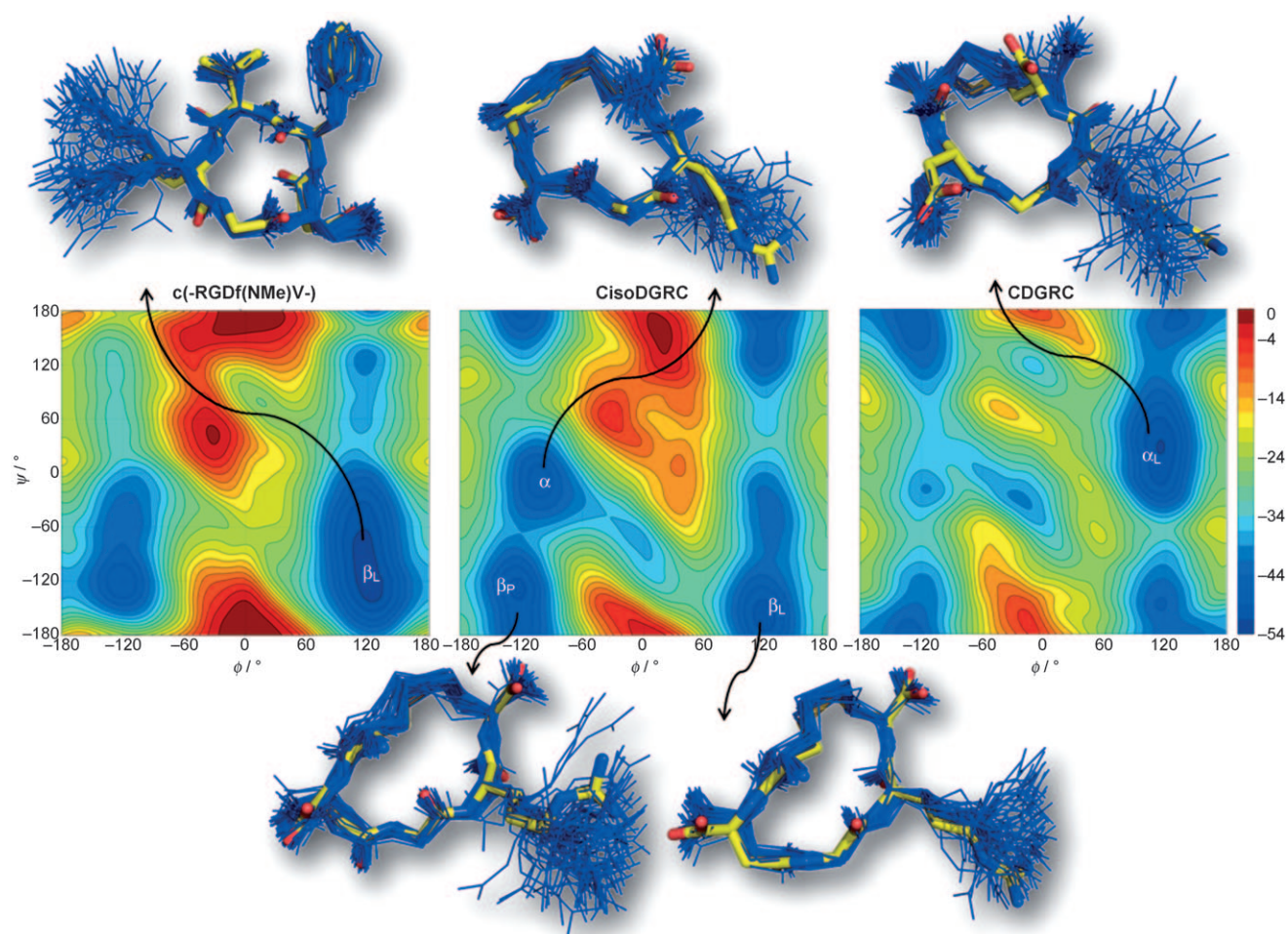


Figure 1. Free-energy surface (FES, kJ mol^{-1}) of c(-RGDf(NMe)V-) (left), CisoDGRC (center), and CDGRC (right) reconstructed by the use of well-tempered MetaD with central Gly ϕ and ψ angles as collective variables (CVs). Each isocontour represents a free-energy difference of 2.5 kJ mol^{-1} . The highest populated FES minima are explicitly labeled. For each peptide, representative bundles of structures extracted from the corresponding FES minima are shown with blue lines, and the center of each cluster is represented by yellow sticks.

distinct regions of the Ramachandran plot^[24] (see Figure S1 in the Supporting Information). To investigate the sampling ability of MetaD on the chosen CVs, we first performed MetaD calculations on c(-RGDf(NMe)V-) and CDGRC, which are well-known high- and low-affinity ligands of $\alpha\beta3$, respectively.^[8,25] Analogous MetaD calculations were then applied to CisoDGRC. The macrocycles displayed different FESs with different minima populations, which implies that the chosen CVs are suitable for the detection of differences in the conformation of the peptides (Figure 1). The FESs of c(-RGDf(NMe)V-) and CDGRC indicate that more than 90% of the structures are contained in the β_L and α_L regions, respectively, whereas CisoDGRC populates the three isoenergetic regions β_L , β_P , and α (Table 1). Interestingly, in the β_L minimum, the Gly ϕ and ψ angles of c(-RGDf(NMe)V-) structures are similar to those observed for the cyclopeptide bound to the $\alpha\beta3$ receptor (Table 1), which is consistent with the fact that the amide groups of Gly and the following residue point in opposite directions.^[26–28] In contrast, in CDGRC this alternate conformation is not fulfilled, which contributes to its inability to bind $\alpha\beta3$.^[25] Finally, CisoDGRC has a high degree of conformational freedom (root-mean-

squared deviation, $\text{RMSD} \approx 1.6 \text{ \AA}$ for the three minima), whereby structures in the β_L and β_P regions adopt an alternate backbone conformation to that in region α (see Figure S2 in the Supporting Information).

To validate the calculations experimentally, we next compared the simulations with NMR spectroscopic data. First, structures extracted from FES minima were compatible with the interresidue ROE (rotating-frame Overhauser effect) values observed for each peptide (see Table S1 in the Supporting Information); furthermore, the minima of the cost function of the contact restraints^[29,30] derived by NMR spectroscopy plotted against the CVs coincided with the minima of the MetaD-calculated free energy (see Figure S3 in the Supporting Information). Second, in an attempt to obtain a quantitative assessment of the accuracy of the calculations, we compared the Gly $^3J_{\text{NH},\text{H}\alpha}$ scalar coupling measured by NMR spectroscopy with the calculated value by using the conformations contained in the FES minima. The direct comparison of experimental NMR spectroscopic data with MetaD simulations relies on the fact that the Gly $^3J_{\text{NH},\text{H}\alpha}$ coupling is a function of the ϕ dihedral angle (as in Karplus-like equations), which is in fact a CV adopted in our MetaD

Table 1: Population distribution and energetic and geometric characteristics of each cyclopeptide in FES minima, as computed by MetaD simulations.

Peptide	Region (ϕ, ψ)	Energy [kJ mol ⁻¹]	Population ^[a] [%]	RMSD ^[b] [Å]	$d_{\text{CG-CZ}}$ ^[c] [Å]	$\theta_{\text{CG-CA-CA}}$ ^[d] [°]
RGDf(NMe)V	β_L	-52.9	97.0	$0.6 \pm 0.2^{[e]}$	12.4 ± 2.0	153.0 ± 8.2
	β_P	-50.4	3.0	$0.5 \pm 0.2^{[e]}$	13.9 ± 1.2	154.4 ± 7.4
CDGRC	β_P	-46.7	8.0	1.1 ± 0.5	10.4 ± 2.1	95.8 ± 8.4
	α_L	-51.7	90.0	0.9 ± 0.4	10.4 ± 0.9	87.1 ± 8.4
CisoDGRC	β_L	-50.2	42.5	0.5 ± 0.2	13.3 ± 0.7	152.4 ± 13.0
	β_P	-50.2	38.3	0.6 ± 0.2	12.5 ± 1.2	111.0 ± 16.4
	α	-47.7	18.4	0.9 ± 0.5	11.3 ± 1.1	89.8 ± 22.0
acCisoDGRC	β_L	-53.1	83.0	0.5 ± 0.2	13.1 ± 1.0	154.3 ± 7.1
	β_P	-50.6	13.5	0.6 ± 0.2	11.1 ± 1.2	101.0 ± 6.6

[a] Population distribution (calculated as described in the Supporting Information) of structures contained in each region. Only minima with a population of more than 2% are reported. [b] RMSD of the bundle of structures contained in each region, as calculated on the basis of the backbone atoms N, CA, C, and O of residues 1–5 and on the basis of the sulfur and CB atoms of residues 1 and 5. [c] $d_{\text{CG-CZ}}$ denotes the distance between the Asp/isoAsp CG and Arg CZ atoms; the measured value in the crystal structure of c(-RGDf(NMe)V-) bound to the $\alpha\beta$ 3 integrin receptor (1L5G) is 13.7 Å.^[28] [d] $\theta_{\text{CG-CA-CA}}$ denotes the angle formed by the Asp/isoAsp CG, Asp/isoAsp CA, and Gly CA atoms; the measured value in the crystal structure of c(-RGDf(NMe)V-) bound to the $\alpha\beta$ 3 integrin receptor (1L5G) is 153.7°.^[28] [e] The RMSD value of the bundle of structures contained in the β_L minimum and the β_P minimum as calculated on the basis of the backbone atoms (N, CA, C, O) of residues 1–5 for the crystal structure of c(-RGDf(NMe)V-) bound to the $\alpha\beta$ 3 integrin receptor (1L5G) is (0.6 ± 0.1) and (0.7 ± 0.1) Å, respectively.

simulations. Importantly, we observed remarkable agreement between the experimental and computed Gly $^3J_{\text{NH,H}\alpha}$ scalar couplings. This agreement confirmed the accuracy of the population distribution of the modeled FES^[31] (see Table S2 in Supporting Information). Third, it is worth noting that interrogating the Dictionary of Protein Secondary Structure (DSSP, <http://swift.cmbi.ru.nl/gv/dssp/>) for Gly ϕ and ψ angles in the RGD and DGR sequences, all Gly ϕ and ψ regions predicted by MetaD are included. Notably, the glycines embedded in the DGR sequence adopt preferentially the ϕ and ψ angles predicted by MetaD (see Figure S1 in the Supporting Information). We therefore concluded that well-tempered MetaD on the chosen CVs is a reliable tool for exploration of the conformational space of this subset of cyclopeptides.

We next investigated the possibility of defining the conformational features that determine the ability of peptides to bind the receptor and thus of discriminating between $\alpha\beta$ 3 binders and nonbinders prior to challenging each ligand with the receptor in vitro. We therefore screened the geometric properties that are dependent on the Gly dihedral angles and affect the distance and reciprocal orientation of the pharmacophoric groups, that is, the Asp/isoAsp carboxylate and the Arg guanidinium group. Remarkably, we identified a close correlation among a) the chosen CVs, b) the distance between CG_{isoAsp/Asp} and CZ_{Arg} ($d_{\text{CG-CZ}}$), which defines the distance between the pharmacophoric groups, c) the reciprocal pharmacophore orientation, which is defined by the angle formed by CG_{isoAsp/Asp}, CA_{Asp}, and CA_{Gly} ($\theta_{\text{CG-CA-CA}}$), and d) the ability of the peptide to interact with the receptor in docking calculations (HADDOCK score).

We analyzed the highest populated FES minima and observed that c(-RGDf(NMe)V-) structures contained in the β_L region adopt an “extended” conformation with $d_{\text{CG-CZ}}$

≈ 13 Å and $\theta_{\text{CG-CA-CA}} \approx 150^\circ$, whereas CDGRC structures in α_L adopt a “contracted” conformation with $d_{\text{CG-CZ}} \approx 10$ Å and $\theta_{\text{CG-CA-CA}} \approx 90^\circ$. Notably, CisoDGRC can adopt both extended (in minimum β_L) and contracted (in minima α and β_P) configurations, in accordance with its high conformational variability (Table 1; see also Figure S4 in the Supporting Information). CDGRC structures extracted from the absolute FES minimum failed to be properly accommodated inside the $\alpha\beta$ 3 binding pocket in docking calculations, conceivably because the contracted distance $d_{\text{CG-CZ}}$ is too short to bridge the α and β integrin domains, and the orientation of the Asp carboxylate is blocked in an unfavorable orientation for coordination of the metal ion, even after the HADDOCK docking semiflexible-refinement step.^[21,22] Conversely,

both c(-RGDf(NMe)V-) and CisoDGRC structures contained in the β_L minimum fit perfectly inside the $\alpha\beta$ 3 binding pocket with a favorable interaction score. These structures, once docked, maintain the original Gly ϕ , ψ , $d_{\text{CG-CZ}}$, and $\theta_{\text{CG-CA-CA}}$ values (see Table S3 in Supporting information), which indicates that conformers contained in the β_L minimum are already in the bioactive form and thus set up to form the canonical ligand/ $\alpha\beta$ 3 contacts (see Figure S5 in the Supporting Information).

Unlike those in the β_L minimum, CisoDGRC structures extracted from the β_P minimum had a closed θ angle. Importantly, during the flexible docking procedure, these structures can dock inside the receptor owing to an opening of the θ angle, which enables reorientation of the Asp carboxylate towards the metal ion. Notably, CisoDGRC contracted structures derived from the α minimum can also dock inside the receptor. However, to optimize the ligand–receptor interactions, they have to significantly change their conformation: the $d_{\text{CG-CZ}}$ distance has to be increased, the $\theta_{\text{CG-CA-CA}}$ angle opened, and the Gly ψ value shifted from the α to the β_P region (see Table S3 and Figure S5 in the Supporting Information).

Overall, these results indicate that conformations that do not require ligand rearrangement for receptor binding reside in the β_L minimum. They provide support for the use of $d_{\text{CG-CZ}}$ (≈ 13 Å), $\theta_{\text{CG-CA-CA}}$ ($\approx 150^\circ$), and Gly ϕ and ψ values as reliable descriptors for the design of RGD/isoDGR-based ligands as potential drugs.

We therefore wondered whether the binding affinity of CisoDGRC for $\alpha\beta$ 3 benefits from chemical modifications that constrain the isoDGR scaffold towards favorable bioactive conformations and thus minimize unfavorable entropic contributions upon binding. To address this issue, we applied MetaD to predict the conformational effects of the

N-terminal acetylation of CisoDGRC ($_{ac}$ CisoDGRC).^[32] MetaD showed that N-acetylation increases the percentage of conformations in the β_L region from around 40 to around 80%, and therefore partially constrains the isoDGR motif towards structures that adopt an extended conformation with appropriate d_{CG-CZ} and $\theta_{CG-CA-CA}$ values for the optimization of ligand–receptor interactions in docking calculations. Furthermore, the presence of the acetyl group in this orientation induces an additional interaction (Table 1 and Figure 2 a; see also Tables S3 and S4 in the Supporting Information). The $_{ac}$ CisoDGRC structures generated by MetaD are compatible with experimental NMR spectroscopic data (see Tables S1 and S2 in the Supporting Information). Finally, to test whether the population increase of the bioactive conformation corresponds to an increase in binding affinity for $_{ac}$ CisoDGRC, we performed binding and competition experiments involving the acquisition of TRNOE (transferred NOE) spectra of living cells^[25] and flow cytometry analysis

of both living cells and $\alpha V\beta 3$ protein (Figure 2 b,c; see also the Supporting Information). Overall, the experimental results indicated that $_{ac}$ CisoDGRC has a greater binding affinity than CisoDGRC.

In conclusion, we have shown that MetaD performed on Gly ϕ and ψ angles reliably described the FES of a relevant set of RGD-, DGR-, and isoDGR-containing cyclopeptides and thus enabled scrutiny of their intrinsic conformational equilibrium and quantitative estimation of the populations of the conformers. Furthermore, these MetaD-generated conformations agree well with experimental data derived by NMR spectroscopy. MetaD can also be successfully applied to predict the effect of chemical modifications on the conformational equilibrium of a molecule. This prediction power is particularly relevant for macrocycles in which conformational heterogeneity can be exploited to fine-tune ligand selectivity and affinity for a specific receptor. In fact, we demonstrated that MetaD can be successfully applied to this class of

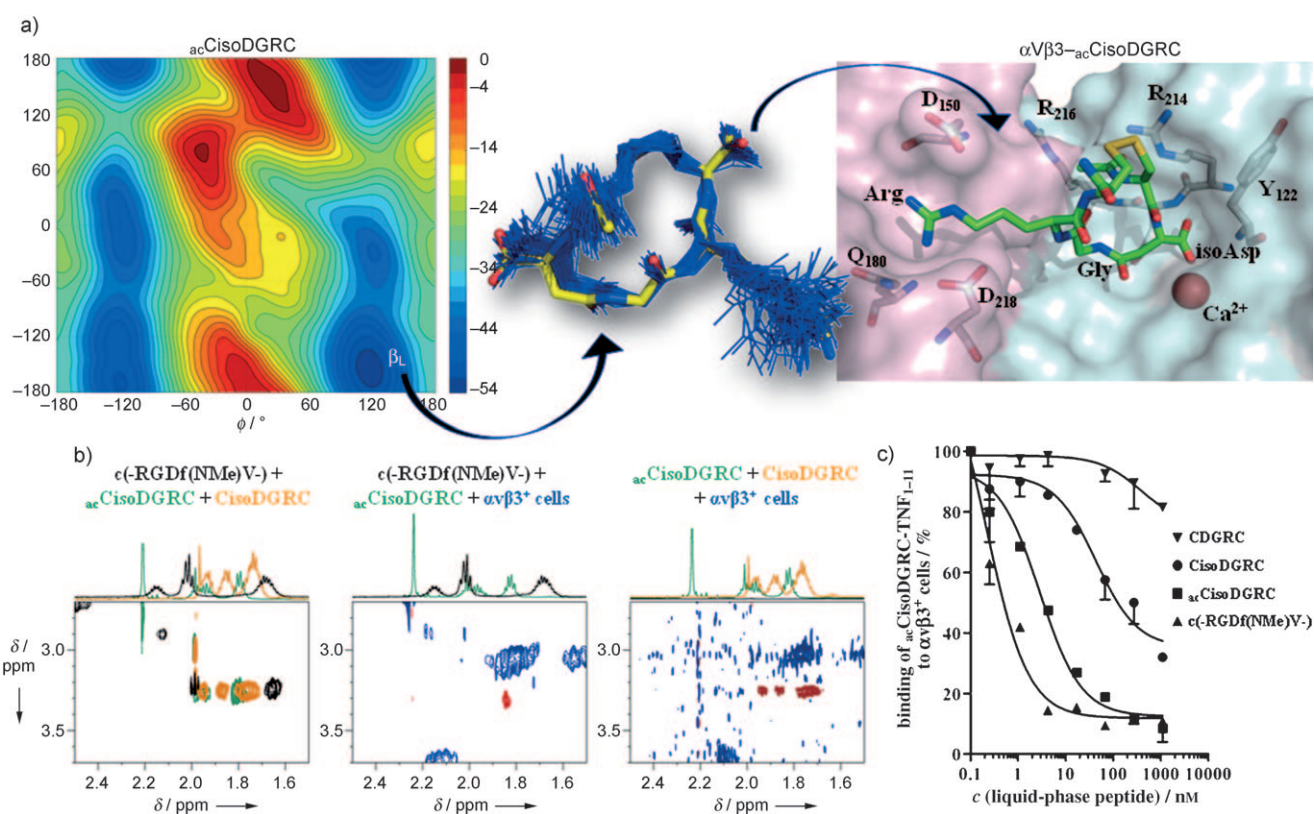


Figure 2. a) Left: FES (kJ mol^{-1}) of $_{ac}$ CisoDGRC reconstructed by using well-tempered MetaD as a function of Gly ϕ and ψ angles. Center: A representative bundle of structures extracted from the FES minimum β_L are shown with blue lines. The center of the cluster within the minimum is represented by yellow sticks. Right: HADDOCK model of the $_{ac}$ CisoDGRC- $\alpha V\beta 3$ binding site. The surfaces of integrin α and β subunits are represented in pink and pale cyan, respectively. The $_{ac}$ CisoDGC side chains interacting with the receptor are shown in green, with nitrogen, oxygen, and sulfur atoms in blue, red, and yellow, respectively. The cation in the metal-ion-dependent adhesion site is represented with a red sphere. The side chains of $\alpha V\beta 3$ and the ligand directly involved in binding are labeled with the one- and three-letter code, respectively. b) Ex vivo TRNOE competition experiments and ligand-affinity ranking. Spectra were acquired as described in the Supporting Information. Top left: Superposition of the 1D ¹H NMR spectra of free c -(RGDf(NMe)V-) (black), CisoDGRC (orange), and $_{ac}$ CisoDGRC (green). Bottom left: Superposition of the NOESY spectra of selected regions of the free ligands. Center: Positive NOE cross-peaks (red) were observed for $_{ac}$ CisoDGRC in the presence of $\alpha V\beta 3^+$ cells and equal amounts of c -(RGDf(NMe)V-); thus, c -(RGDf(NMe)V-), which has the highest relative affinity, displaced $_{ac}$ CisoDGRC from $\alpha V\beta 3$. Right: A stoichiometric mixture of CisoDGRC and $_{ac}$ CisoDGRC was added to $\alpha V\beta 3^+$ cells. The observation of positive NOE cross-peaks for CisoDGRC, which must be free in solution, indicated that $_{ac}$ CisoDGRC has the highest relative affinity and is therefore able to displace CisoDGRC. c) Competitive binding of biotinylated $_{ac}$ CisoDGRC-TNF₁₋₁₁ (TNF = tumor necrosis factor) to $\alpha V\beta 3^+$ cells in the presence of $_{ac}$ CisoDGRC, CisoDGRC, CDGRC, or c -(RGDf(NMe)V-) at increasing concentrations, c . Flow cytometry analyses were carried out as described in the Supporting Information.

peptides to generate reliable structural models that can be docked inside the receptor. The combination of both MetaD and docking enables the discrimination of binding and nonbinding cyclopeptides and prediction of the effect of flanking residues, and contributes to the definition of descriptors for good ligands and the ability to rapidly discard “unproductive” ligands in silico. Accordingly, the exclusion of unproductive conformations resulted in the observed increased affinity of $_{ac}$ CisoDGRC over CisoDGRC in competition experiments. Overall, these findings provide support for the application of MetaD/docking as an innovative technique combination to improve the rational design of isoDGR-based diagnostic and therapeutic agents along with the rapid and accurate screening of peptide libraries. Finally, it is conceivable that the coupling of MetaD to docking could be successfully exploited for other ligand–receptor systems following the identification of appropriate CVs to characterize the ligand conformational ensemble.

Received: November 11, 2010

Published online: January 18, 2011

Keywords: conformational sampling · drug design · metadynamics · molecular dynamics · receptor–ligand interactions

- [1] J. S. Desgrosellier, D. A. Cheresh, *Nat. Rev. Cancer* **2010**, *10*, 9–22.
- [2] A. Corti, F. Curnis, W. Arap, R. Pasqualini, *Blood* **2008**, *112*, 2628–2635.
- [3] C. Rüegg, G. C. Alghisi, *Recent Results Cancer Res.* **2010**, *180*, 83–101.
- [4] K. E. Gottschalk, H. Kessler, *Angew. Chem.* **2002**, *114*, 3919–3927; *Angew. Chem. Int. Ed.* **2002**, *41*, 3767–3774.
- [5] F. Curnis, R. Longhi, L. Crippa, A. Cattaneo, E. Dondossola, A. Bachi, A. Corti, *J. Biol. Chem.* **2006**, *281*, 36466–36476.
- [6] A. O. Frank, E. Otto, C. Mas-Moruno, H. B. Schiller, L. Marinelli, S. Cosconati, A. Bochen, D. Vossmeier, G. Zahn, R. Stragies, E. Novellino, H. Kessler, *Angew. Chem.* **2010**, *122*, 9465–9468; *Angew. Chem. Int. Ed.* **2010**, *49*, 9278–9281.
- [7] G. Pathuri, K. Sahoo, V. Awasthi, H. Gali, *Bioorg. Med. Chem. Lett.* **2010**, *20*, 5969–5972.
- [8] A. Spitaleri, S. Mari, F. Curnis, C. Traversari, R. Longhi, C. Bordignon, A. Corti, G. P. Rizzardi, G. Musco, *J. Biol. Chem.* **2008**, *283*, 19757–19768.
- [9] A. Liwo, C. Czaplewski, S. Oldziej, H. A. Scheraga, *Curr. Opin. Struct. Biol.* **2008**, *18*, 134–139.
- [10] W. F. van Gunsteren, J. Dolenc, A. E. Mark, *Curr. Opin. Struct. Biol.* **2008**, *18*, 149–153.
- [11] T. Huber, A. E. Torda, W. F. van Gunsteren, *J. Comput.-Aided Mol. Des.* **1994**, *8*, 695–708.
- [12] D. Cvijovicacute, J. Klinowski, *Science* **1995**, *267*, 664–666.
- [13] F. Wang, D. P. Landau, *Phys. Rev. Lett.* **2001**, *86*, 2050–2053.
- [14] E. Darve, A. Pohorille, *J. Chem. Phys.* **2001**, *115*, 9169–9183.
- [15] H. Grubmüller, *Phys. Rev. E* **1995**, *52*, 2893–2906.
- [16] G. N. Patey, J. P. Valleau, *J. Chem. Phys.* **1975**, *63*, 2334–2339.
- [17] A. M. Ferrenberg, R. H. Swendsen, *Phys. Rev. Lett.* **1988**, *61*, 2635–2638.
- [18] P. G. Bolhuis, D. Chandler, C. Dellago, P. L. Geissler, *Annu. Rev. Phys. Chem.* **2002**, *53*, 291–318.
- [19] A. Laio, F. L. Gervasio, *Rep. Prog. Phys.* **2008**, *71*, 126601.
- [20] A. Laio, M. Parrinello, *Proc. Natl. Acad. Sci. USA* **2002**, *99*, 12562–12566.
- [21] S. J. de Vries, A. D. van Dijk, M. Krzeminski, M. van Dijk, A. Thureau, V. Hsu, T. Wassenaar, A. M. Bonvin, *Proteins Struct. Funct. Genet.* **2007**, *69*, 726–733.
- [22] C. Dominguez, R. Boelens, A. M. Bonvin, *J. Am. Chem. Soc.* **2003**, *125*, 1731–1737.
- [23] A. Barducci, G. Bussi, M. Parrinello, *Phys. Rev. Lett.* **2008**, *100*, 020603.
- [24] B. K. Ho, R. Brasseur, *BMC Struct. Biol.* **2005**, *5*, 14.
- [25] S. Mari, C. Invernizzi, A. Spitaleri, L. Alberici, M. Ghitti, C. Bordignon, C. Traversari, G. P. Rizzardi, G. Musco, *Angew. Chem.* **2010**, *122*, 1089–1092; *Angew. Chem. Int. Ed.* **2010**, *49*, 1071–1074.
- [26] T. Cupido, J. Spengler, J. Ruiz-Rodriguez, J. Adan, F. Mitjans, J. Piulats, F. Albericio, *Angew. Chem.* **2010**, *122*, 2792–2797; *Angew. Chem. Int. Ed.* **2010**, *49*, 2732–2737.
- [27] M. A. Dechantsreiter, E. Planker, B. Matha, E. Lohof, G. Holzemann, A. Jonczyk, S. L. Goodman, H. Kessler, *J. Med. Chem.* **1999**, *42*, 3033–3040.
- [28] J. P. Xiong, T. Stehle, R. Zhang, A. Joachimiak, M. Frech, S. L. Goodman, M. A. Arnaout, *Science* **2002**, *296*, 151–155.
- [29] G. Fiorin, A. Pastore, P. Carloni, M. Parrinello, *Biophys. J.* **2006**, *91*, 2768–2777.
- [30] C. D. Schwieters, J. J. Kuszewski, N. Tjandra, G. M. Clore, *J. Magn. Reson.* **2003**, *160*, 65–74.
- [31] V. Spiwok, I. Tvaroska, *Carbohydr. Res.* **2009**, *344*, 1575–1581.
- [32] F. Curnis, A. Cattaneo, R. Longhi, A. Sacchi, A. M. Gasparri, F. Pastorino, P. Di Matteo, C. Traversari, A. Bachi, M. Ponzoni, G. P. Rizzardi, A. Corti, *J. Biol. Chem.* **2010**, *285*, 9114–9123.